UNLIMITED

RSRE
MEMORANDUM No. 4290

ROYAL SIGNALS & RADAR ESTABLISHMENT

TITANIUM-DOPED SAPPHIRE LASERS WITH HIGH ENERGY PUMPING

Authors: M J P Payne & N A Lowde

PROCUREMENT EXECUTIVE,
MINISTRY OF DEFENCE,
RSRE MALVERN,
WORCS.

RSRE MEMORANDUM No. 4290

UNLIMITED

C056317

CONDITIONS OF RELEASE

BR-112067

****

U

****

Y

Reports quoted are not necessarily available to members of the public or to commercial organisations.

ROYAL SIGNALS AND RADAR ESTABLISHMENT

Memorandum 4290

TITLE: TITANIUM-DOPED SAPPHIRE LASERS WITH HIGH ENERGY PUMPING

AUTHORS: M J P Payne and N A Lowde

DATE: June 1989

SUMMARY

A titanium-doped sapphire is pumped with up to 900 mJ of blue-green energy from a dye laser. 8% energy conversion to the near IR is demonstrated. The experimental input/output data agree well with calculations based on the measured characteristics of crystal and pump beam. Analysis of the conversion efficiency reveals the potential to achieve values of about 35% in optimised, but simple, devices.

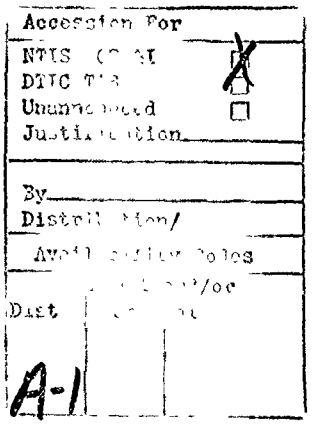

TITANIUM-DOPED SAPPHIRE LASERS WITH HIGH ENERGY PUMPING

M J P Payne and N A Lowde

A laser rod of titanium-doped sapphire was supplied by Naval Research Laboratory (NRL) to RSRE. The crystal was characterised spectroscopically and was tested in its laser action. The laser experiments were conducted using a flashlamp-pumped dye laser (FPDL) as the pump source. The FPDL emitted up to 1.8 J in a 3 μs pulse at 490 nm wavelength. The purpose of this experiment was to effect an approximate simulation of Ti:sapphire lasing with a powerful frequency-doubled neodymium laser as pump and thus to assess the usefulness of such a combination.

Another crystal of Ti:sapphire, which was less heavily doped, was tested in the same manner. This crystal was supplied by Air Force Weapons Avionics Laboratory (AFWAL).

CRYSTAL CHARACTERISATION

The crystals from both NRL and AFWAL took the form of cylinders with ground barrel surfaces and ends polished to laser standards.

The material as supplied had no dielectric coatings. Both rods were anti-reflection coated (in the UK) for both the 490 nm pump wavelength and the 750-850 nm lasing band.

The fluorescence of the crystals was assessed by observation of the emission spectrum under argon laser pumping (488 nm) and the fluorescence decay following excitation by a 3 ns dye laser pulse (450 nm). None of these observations showed any unexpected features. The fluorescence decays were measured at room temperature (23°C) and revealed a single exponential decay extending over at least three decades of signal amplitude and with time constants close to 3.3 μs.

The optical absorption in the visible pump band and in the near IR emission band was measured on a Cary 14 spectrophotometer. The optical loss at 800 nm, close to the lasing wavelength, was measured using a laser diode. The numerical results relevant to lasing are given in Table 1.

Again, there is nothing unusual in the results. The NRL sample has a rather low figure of merit but this is not unexpected because the crystal is an early sample of quite highly doped material.

It is noted that both crystals exhibit the beneficial combination for π-polarised radiation of largest absorption in the visible with largest optical gain coefficient and smallest absorption in the infra-red.

Using the value of absorption cross section derived by P Moulton ($6.5\ 10^{-20} cm^2$ for peak value for π-polarisation) the density of Ti^{3+} ions in each crystal may be calculated, with the results shown in Table 1. We have some reason to believe Moulton's value to be a factor of about two too low. In this case the tabulated doping densities are too high by the same factor. The values in the last three rows of Table 1 also depend on the same factor.

Table 1. Optical Properties of Ti:Sapphire Samples

Source of crystal	NRL	AFWAL
Serial No of crystal	ID57	None
Length/mm	31.0	18.8
Fluorescence decay time/μs	3.3	3.3
Optical absorbance at 490 nm		
π-polarisation	0.92	0.28
σ-polarisation	0.405	0.123
Optical transmission at 490 nm		
π-polarisation	0.120	0.525
σ-polarisation	0.394	0.753
Absorption of unpolarised radiation at 490 nm	0.743	0.361
Absorption coefficient at 490 nm (π-polarisation)/cm^{-1}	0.684	0.343
Optical transmission at 800 nm		
π-polarisation	0.925	0.9917
σ-polarisation	0.882	0.988
Figure of merit ($\alpha_{490}/\alpha_{800}$)	27.2	80
Estimated density of Ti^{3+} ions/cm^{-3}	$1.05.10^{19}$	$5.3.10^{18}$
Stored energy for full inversion /Jcm^{-3}	2.60	1.31
/Jcm^{-2}	8.1	2.5
Input power at 490 nm to maintain 50% inversion/kw cm^{-3}	1290	650

LASER EXPERIMENTS

The titanium:sapphire laser resonator was formed by two plane mirrors as shown in Figure 1. The distance between the mirrors was 12 cm. The crystal was pumped by means of a flashlamp-pumped dye laser (FPDL) by transmission through the dichroic left-hand resonator mirror. This mirror was totally reflecting in the spectral range 750 to 900 nm and 95% transmitting at the 490 nm output wavelength of the dye laser. The second mirror exhibited 53% reflection at the Ti:sapphire output wavelength near 800 nm and 15% reflection at 490 nm. Thus very little of any pump radiation not absorbed by the crystal on its first pass was reflected back to the crystal. The dye laser output beam, which had a circular cross-section of diameter 10 mm, was condensed into the crystal by means of a lens with 50 cm focal length. The crystal was placed some distance before the focus to minimise the chances of optically induced damage. The pumping density was altered by adjusting the crystal position relative to the focus. In our experiments the pump beam diameter at the crystal input face was typically 3 mm and changed little through the length of the crystal.

The output pulse of the dye laser was unpolarised and had a duration of 3 μs (between times at ¼ peak power). Repetition rate was very low, essentially single shot. The FPDL employed a solution of coumarin 490 dye in methanol.

To ensure constancy in the pump beam profile and pulse length for a range of pump energies to the sapphire crystal, the dye laser was always fired at maximum output and the output was attenuated by the desired degree using neutral density glass filters. Thus the input-output characteristic of the Ti:sapphire laser was determined.

The output energy of the sapphire laser was measured using a Scientech energy meter after the removal of residual pump radiation by means of an OG610 glass filter.

In associated experiments a silicon photodiode was employed to observe, respectively, the pump pulse shape, the output pulse shape and the side fluorescence from the sapphire crystal with and without lasing.

RESULTS

With the NRL sapphire crystal positioned so that the beam entering the crystal had an elliptical cross-section 3 mm x 4 mm (as measured from a burn mark on exposed Polaroid film) the input-output curve was as shown in Figure 2. Additional data were obtained with both crystals positioned somewhat closer to the pump beam focus. (Figures 3 and 4) The two positions were with the crystal entrance face at 11.6 cm and 5.3 cm respectively from the lens focus and are designated Positions 1 and 2.

The pulse forms of the pump pulse, sapphire laser output pulse and sapphire fluorescence with and without laser action are shown in Figures 5 to 8 respectively.

ANALYSIS OF LASING ACTION

In order to extrapolate from the experimentally achieved results to the performance expected under other operating conditions, and to optimise performance, it is necessary to model the properties of the Ti:sapphire laser as it stands. Such modelling is reasonably straightforward in terms

of the electronic structure of the laser crystal. It is complicated in the present case by two main factors. The first of these is the non-uniformity of the pump beam profile (Figure 9). The second factor is the similarity between the length of the pump pulse and the fluorescence decay time of the Ti^{3+}. This leads to a dependence of laser performance on the detailed shape of the pump and fluorescence pulses.

The symbols employed in the performance analysis are defined in Table 2.

i. Pump Beam Profile Effects.

The pump beam profile measured at the input face of the crystal in position 2 is shown in Figure 9. This reveals that there is a strong central lobe of radius about 1¼ mm, a low intensity tail extending to at least 4 mm from beam axis and a narrow ring of radius 2.5 mm.

For a pump pulse of total energy ϕE_a the pump fluence on axis can be derived from Figure 9. Its value is

$$\varepsilon_a = 5.15\ \phi\ E_a\ \text{Jcm}^{-2} \qquad (1)$$

(This takes into account the slight ellipticity of the beam cross-section and the slight shift in sample position from the beam measurement plane.)

The central lobe of the beam carries 46% of the total energy. Since excitation by the low intensity tail is likely to be ineffective in laser action, we assume that only 46% of the input can possibly give rise to laser output. This is confirmed in practice.

ii. Pump Pulse Length Effects.

Regarding temporal effects, consider a pump beam incident on the laser crystal in a pulse with power P(t). With no laser action (and no saturation of Ti absorption) the resulting stored energy in the upper laser energy level is

$$\varepsilon_e(t) = \int_0^t P(t')\exp(-(t-t')/\tau_o)dt' \quad x(\lambda_p/\lambda_f) \qquad (2)$$

where τ_o is the fluorescence decay time, λ_p and λ_f are the wavelengths of the pump and fluorescence radiation. $\varepsilon_e(t)$ represents the excitation integrated over the length of the laser crystal. The small signal gain, g, for single pass of the crystal is $\varepsilon_e(t)/\varepsilon_{sat}$. ε_{sat}, the saturation fluence, has the value 0.9 Jcm^{-2}. The small signal gain is readily related to laser threshold by the measured values of the various resonator losses.

The time dependence of pumping and lasing is modelled using the experimentally determined pump and fluorescence pulse forms shown in Figure 10. This leads to values for the excitation available for lasing and hence to theoretical values for the output slope efficiency. Schematically the situation is shown in Figure 11. The pump pulse of Figure 11(a) generates excitation following Figure 11(b) if no lasing occurs. The crystal fluorescence follows Figure 11(b) also. Maximum excitation occurs at time T_o and, with pumping just above threshold, laser output appears at this time. For a particular pump pulse shape the peak value of excitation may be derived from equation (2). The most useful expression of peak excitation energy/unit area of laser rod cross-section is as a ratio with

Table 2. Symbols for Laser Performance Calculations

Total energy from dye laser	=	E_d	1.3 J
Total energy through aperture	=	E_a	810 mJ
Pump attenuator transmission	=	ϕ	
Total energy at dichroic mirror (pump energy)	=	$e_p = \phi E_a$	
Dichroic mirror transmission for pump	=	ρ	= 0.95
Total energy at crystal input face	=	$e_{in} = \rho\phi E_a$	
On-axis fluence at crystal input face	=	$\varepsilon_{in} = 5.15\ \rho\phi E_a$	
Energy in central lobe at crystal input face	=	$e_i = \kappa e_{in}$	
Crystal optical absorption for unpolarised radiation	=	β	= 0.743
Absorbed energy from central lobe	=	$e_{abs} = \beta e_i$	
Absorbed fluence on-axis	=	$\varepsilon_{abs} = \beta\varepsilon_{in}$	
Instantaneous absorbed intensity	=	$P(t)$	
Instantaneous excitation/cm^2	=	$\varepsilon_e(t)$	
Total excitation in crystal from central lobe	=	$e_1 = \lambda_p/\lambda_f\ e_i$	
Extractable excitation	=	e_x	
Peak excitation/cm^2 on axis	=	$\varepsilon_o = \lambda_p/\lambda_f\ \gamma\varepsilon_{abs}$	
Threshold excitation/cm^2 on axis	=	ε_T	
Saturation fluence	=	ε_{sat} =	900 mJ/cm^2
Laser output energy	=	e_{out}	
Threshold pump energy (at dichroic mirror)	=	e_{thr}	

the total fluence of the pump pulse, ie the quantity γ where

$$\gamma = \varepsilon_o / \varepsilon_{abs} \quad (3)$$

Figure 11 shows the situation also for pumping above threshold. Specifically the case for pumping at twice threshold is depicted, when the vertical scales of Figures 11(a) and 11(b) would be doubled from those for threshold. The excitation rises to its lasing threshold value at time T_1. The excitation is then clamped at this level during lasing (Figure 11(c)). Note that this clamping of the fluorescence output during lasing is not evident in Figure 7 because of the limited proportion of the total excitation which is actually available for lasing due to pump beam inhomogeneity.

The excess of pump power over fluorescence emission represents the power instantaneously available for lasing. (We assume that energy extraction by lasing takes place very quickly.) Lasing continues until the pump power falls to equal the excitation loss by spontaneous decay at the threshold excitation level. This happens at time T_2. The value of T_2 can be derived from the shape of the pump pulse as shown in Figure 11(a). Note that, at threshold, power P_o is the input required to balance fluorescence losses.

Times T_1 and T_2 clearly depend on the pumping ratio (input energy/threshold input energy) and on the pump pulse shape. In our experiments, as explained earlier, the pump pulse shape was maintained constant for all pump energies.

The energy available for lasing is that delivered by the pump between times T_1 and T_2 and in excess of that required to supply fluorescence and non-radiative losses. This energy is represented by the shaded area in Figure 11(a). The laser output pulse shape is shown in Figure 11(d). The energy actually delivered as laser output depends on the output coupling efficiency.

Table 3 shows the expected values of T_1, T_2 and available excitation as a function of the pumping ratio. These data are derived from the measured pump and fluorescence pulse shapes of Figure 10 using the scheme described above. It was found that the pump pulse shape could be well represented by the expression

$$P(t) = P_o . t/\tau_p . \exp(-t/\tau_p) \quad (4)$$

with τ_p = 0.83 μs. The integration in equation (2) could then be performed analytically and the value of maximum excitation (γ in equation (3)) thus calculated. Taking the crystal fluorescence decay time, τ_o, to be 3.3 μs, then

$$\gamma = 0.55\ \lambda_p/\overline{\lambda}_f \quad (5)$$

CALCULATION OF LASING THRESHOLD AND SLOPE EFFICIENCY

The initial calculation below refers to our most reliable data (NRL sample in Position 1; Figure 2).

i. Lasing Threshold.

Since the excitation is greatest on the pump beam axis, it is expected that threshold lasing will occur in this part of the crystal.

Table 3. Extractable Energy, e_x, as function of Pumping Ratio

Pumping Ratio E_p/E_{thr}	$T_1/\mu s$	$T_2/\mu s$	$e_x/e_{thr} \times \lambda_f/\bar{\lambda}_p$	e_x/e_{thr} $\left\{ \begin{array}{l} \bar{\lambda}_f = 800nm \\ \lambda_p = 490nm \end{array} \right.$
1.1	1.76	2.37	0.034	0.021
1.2	1.56	2.48	0.145	0.089
1.5	1.27	2.70	0.334	0.205
2	1.04	3.03	0.705	0.432
3	0.80	3.49	1.53	0.937
4	0.66	3.81	2.52	1.54
6	0.50	4.25	4.53	2.77
10	0.35	4.80	8.69	5.32

The peak value of small signal optical gain on axis is

$$g_o = \varepsilon_o/\varepsilon_{sat}$$

In terms of the total input energy incident on the Ti:sapphire laser dichroic mirror and using equation 1 and the data of Table 2

$$g_o = 5.15\ \rho\gamma\beta.\lambda_p/\bar{\lambda}_f\ e_p/\varepsilon_{sat}$$

$$= 1.36\ e_p$$

The resonator losses arise from the output ($\ln(R) = -0.635$) and the absorption (at 800 nm and for π-polarisation) in the crystal ($\alpha l = 0.075$ per single pass). The total round trip loss coefficient is

$$2\alpha\ l - \ln(R) = 0.785 = L$$

At threshold

$$2g_o = L$$

Hence $e_{thr,calc} = 288$ mJ

ii. Lasing Slope Efficiency.

Calculation of the slope efficiency may be treated similarly. In the limit of pumping at many times threshold, and ignoring saturation effects, all of the excitation above the threshold value is potentially available for lasing. The output coupling coefficient for the Ti:sapphire laser is

$$C = -\ln(R)/L = 0.803.$$

The limiting value of slope efficiency, η, is then

$$\eta_{calc} = C\ \beta\ \lambda_p/\bar{\lambda}_f\ \kappa\rho$$

$$= 0.160$$

The values thus calculated for lasing threshold and the slope efficiency are in excellent agreement with experiment, as shown by Figure 2. The curve of Figure 2 is derived from these values, used in combination with the calculations on temporal dependence summarised in Table 3.

Similar calculations have been performed for the remaining laser results currently available, ie for both NRL and AFWAL samples in crystal position 2 with a rather greater degree of pump focussing. The data in these cases are known to be less good due to significant (25%) fluctuations in the dye laser output. The calculated values are compared in Table 4 with those derived from the best achievable curve fitting to the experimental data.

Table 4.

Crystal	Sample Position	Threshold energy/mJ calc	exp	Limiting slope calc	exp	
NRL	1	288	290	0.160	0.160	
NRL	2	150	150	0.160	0.14	
			or 230		0.21	- apparently a better fit
AFWAL	2	250	250	0.095	0.035	
			or 330		0.046	- apparent best fit

POTENTIAL FOR EFFICIENCY IMPROVEMENT

We have shown that good agreement can be obtained between the measured performance of a titanium-doped sapphire laser with a monochromatic, 3 microsecond pump pulse and the performance calculated from the temporal and spatial properties of the pump pulse together with the spectroscopic properties of the laser crystal. The characterisation of this laser and its pumping system may be considered to be complete for the present purposes; there appear to be no major unquantifiable properties. It therefore remains only to estimate the performance enhancement which might be expected through improvements in the pump laser or laser crystal.

The question of performance improvement is best tackled by more clearly identifying the losses in efficiency due to each of the deficiencies mentioned earlier. Table 5 shows the five main factors contributing to the loss of laser output and indicates the energy efficiency for each process and the cumulative efficiency.

Table 5. Lasing Efficiency for NRL Sample (Position 1)

		Energy Efficiency	Cumulative Efficiency
1.	Quantum defect	0.61	0.61
2.	Absorbed fraction of pump energy	0.75	0.46
3.	Output coupling efficiency	0.80	0.37
4.	Pump pulse duration effects (at 3 x threshold)	0.51	0.19
5.	Pump beam profile effects	0.46	0.087

Table 5 reveals the major loss in efficiency due to the properties of the pump beam. The combined temporal and spatial pump beam effects amount to a laser output reduction by a factor of more than four. The use of more recently produced crystals with higher doping concentration would increase the pump absorption; the effect of doubling the concentration is to change 0.75 to 0.90 in Table 5, line 2. The same effect might be achieved by increase of crystal length, but with parallel increase in the absorption loss for lasing. The use of modern crystals, with their much reduced loss coefficient in the lasing spectral band, would yield significant improvement in output coupling efficiency (line 3) to a value of perhaps about 0.9 even with optimisation of the output mirror reflectivity (to around 0.75 to 0.8). These changes should result in a significant reduction in lasing threshold by a factor of roughly 2, with increase in the pumping ratio (pump energy/threshold energy) by the same factor. The value of 3 for pumping ratio used in Table 5, line 4 would thereby be increased to 6, with consequent increase in laser efficiency for temporal effects from 0.51 to 0.75 (derived from Table 3).

Furthermore, if the pump pulse length were reduced from the present 3 μs to a value much less than the fluorescence lifetime of the titanium, then the threshold energy would be reduced by a factor 0.55 (the numerical factor in equation 5) and the temporal effects efficiency would increase to roughly the value $(1 - 0.55/6) \simeq 0.91$. In this case, the cumulative efficiency up to line 4 of Table 5 is $0.61 \times 0.90 \times 0.80 \times 0.91 = 0.40$.

The short pulse pumping just mentioned would generally be achieved by the use of a frequency doubled neodymium laser emitting near 530 nm wavelength. In this case the efficiency value for Table 5, line 1 would be increased to $530/800 = 0.66$. Since the optical absorption coefficient would be appreciably reduced at the new pump wavelength, care would be needed to maintain a high value of pump light absorption.

The last line of Table 5 depends on the degree of pumping uniformity which can be achieved without sacrifice of pump energy. This is principally a matter of pump laser design. We may note that the near field output beam from the dye laser used in these experiments has good uniformity before the beam condensing lens. Also, the Hyper YAG series of neodymium lasers available from Lumonics Ltd delivers a suitable "top-hat" beam profile. In general, it is likely that a uniform pump beam profile could be derived from most pump lasers by the use of a slightly tapered light guide having a bend (of around 90°) for "ray-mixing". By such means the inefficiency represented by Table 5, line 5 may be reduced. The current efficiency value of 0.46 may perhaps be replaced by 0.8. The overall titanium:sapphire lasing efficiency would then reach a value of about 0.35. This figure agrees with that obtained by Moulton (unpublished) and others for pumping by frequency-doubled Nd:YAG lasers.

CONCLUSION

Conversion of dye laser output into the near infrared by the use of a titanium:sapphire laser has been demonstrated with about 8% energy efficiency. This performance has been accurately modelled using the measured properties of the crystal and pump beam. Conversion efficiency of about 35 to 40% appears to be readily achievable with an optimised system. 30% slope efficiency values have been reported by several workers using frequency-doubled Nd:YAG pumps but at much lower energy than in our experiments. The sapphire laser in this case may be very simple; just a short crystal (around 2 cm in length) with suitable end dielectric

coatings. The specific output wavelength (near 800 nm) may be selected by variation of the dielectric coating. We have not investigated the beam divergence properties of such a laser.

ACKNOWLEDGEMENTS

We are grateful to Dr R Burnham (formerly of Naval Research Laboratory) and Dr K Schepler (Wright Patterson Air Force Base) for supply of the titanium:sapphire crystals; to G Cook (RAE Farnborough) for provision of (and practical assistance with) the dye laser; to H W Evans (RSRE) for practical help and useful discussions.

FIGURE.1 LASER - PUMPED TITANIUM: SAPPHIRE LASER (SCHEMATIC)

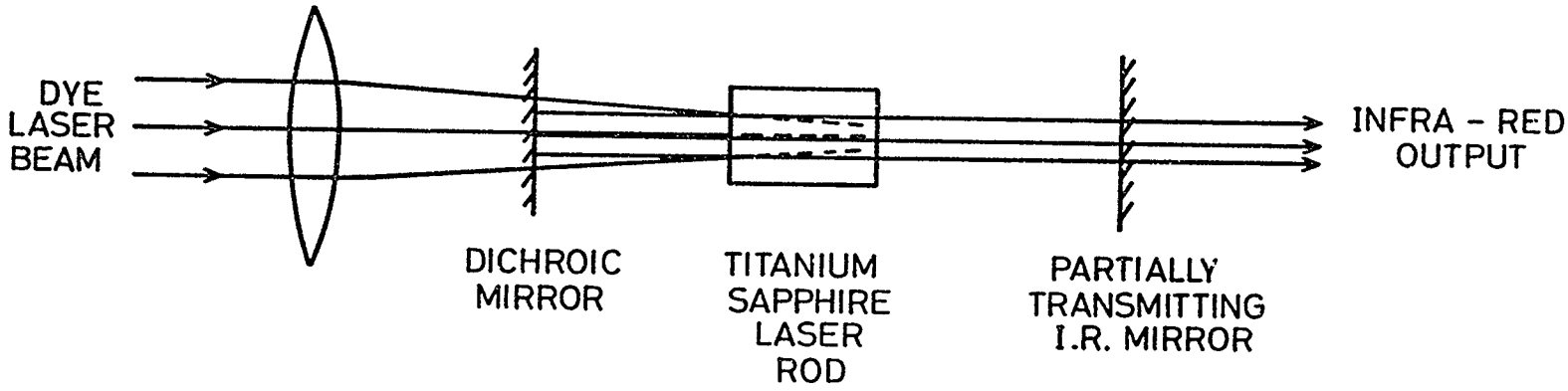

INITIAL RESULTS - INPUT ENERGY 800mJ IN 3μs PULSE
OUTPUT ENERGY 100 mJ

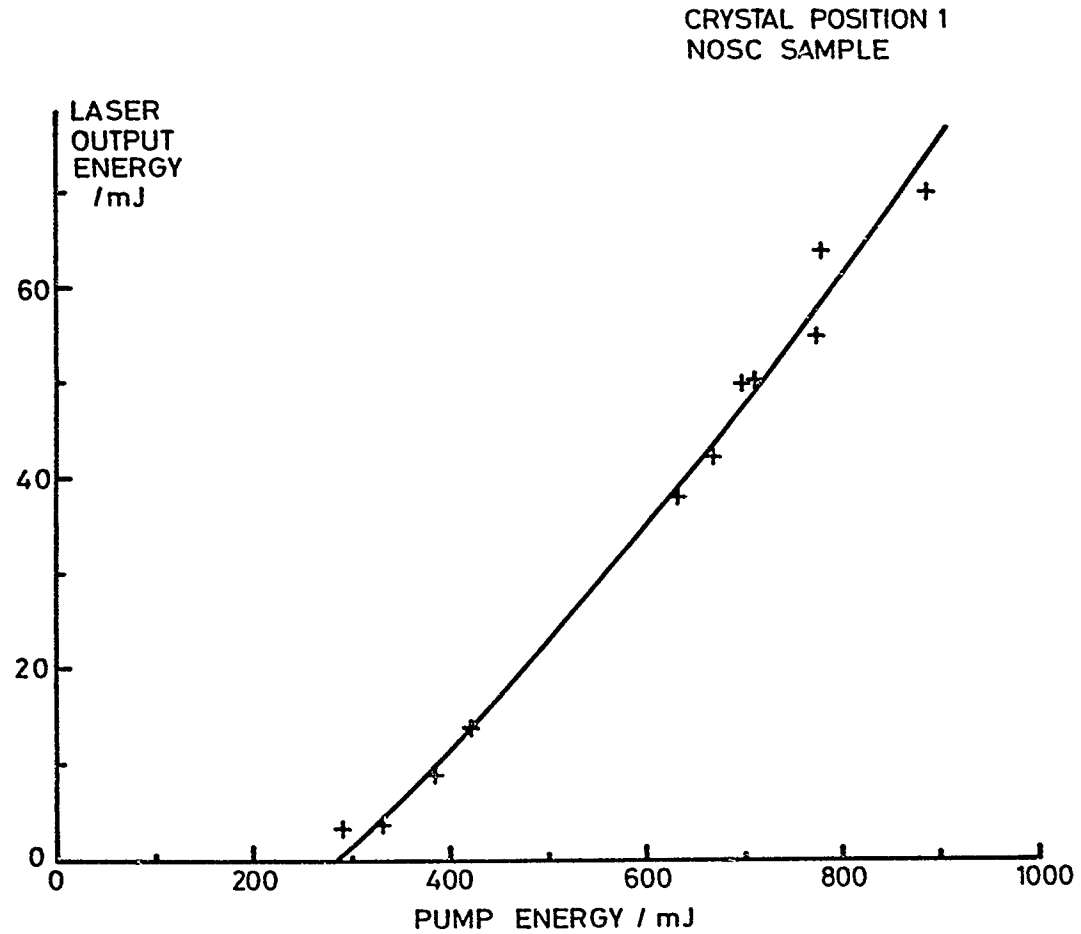

FIGURE. 2 Ti : SAPPHIRE LASING

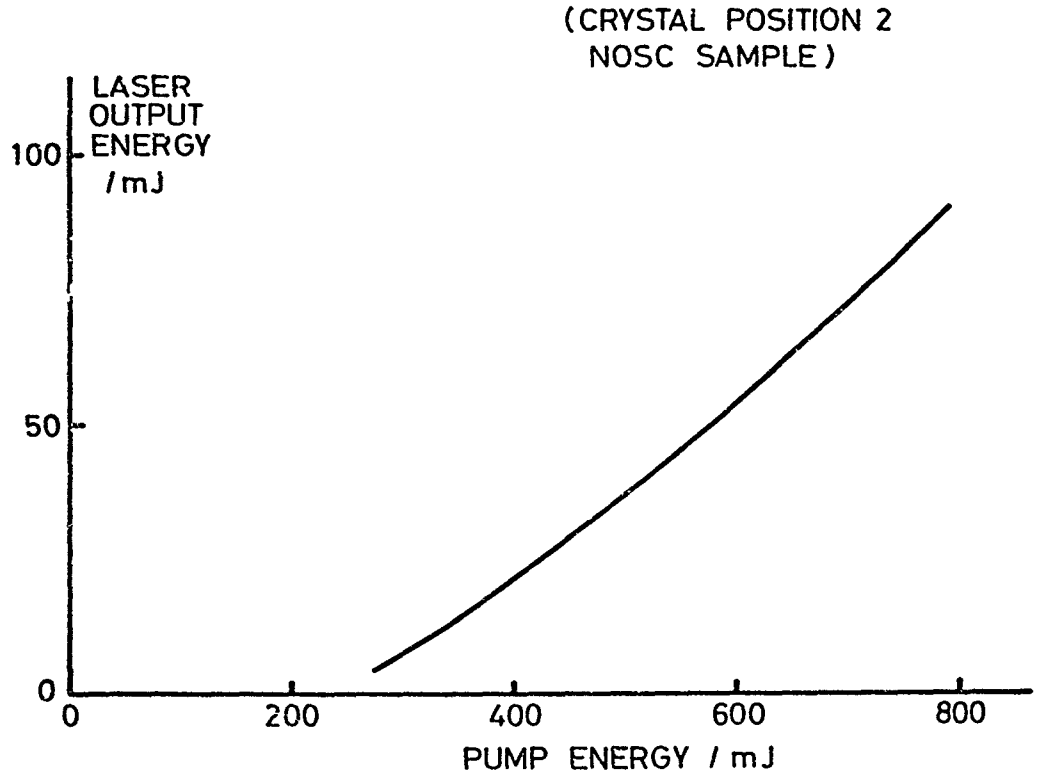

FIGURE. 3 Ti : SAPPHIRE LASING

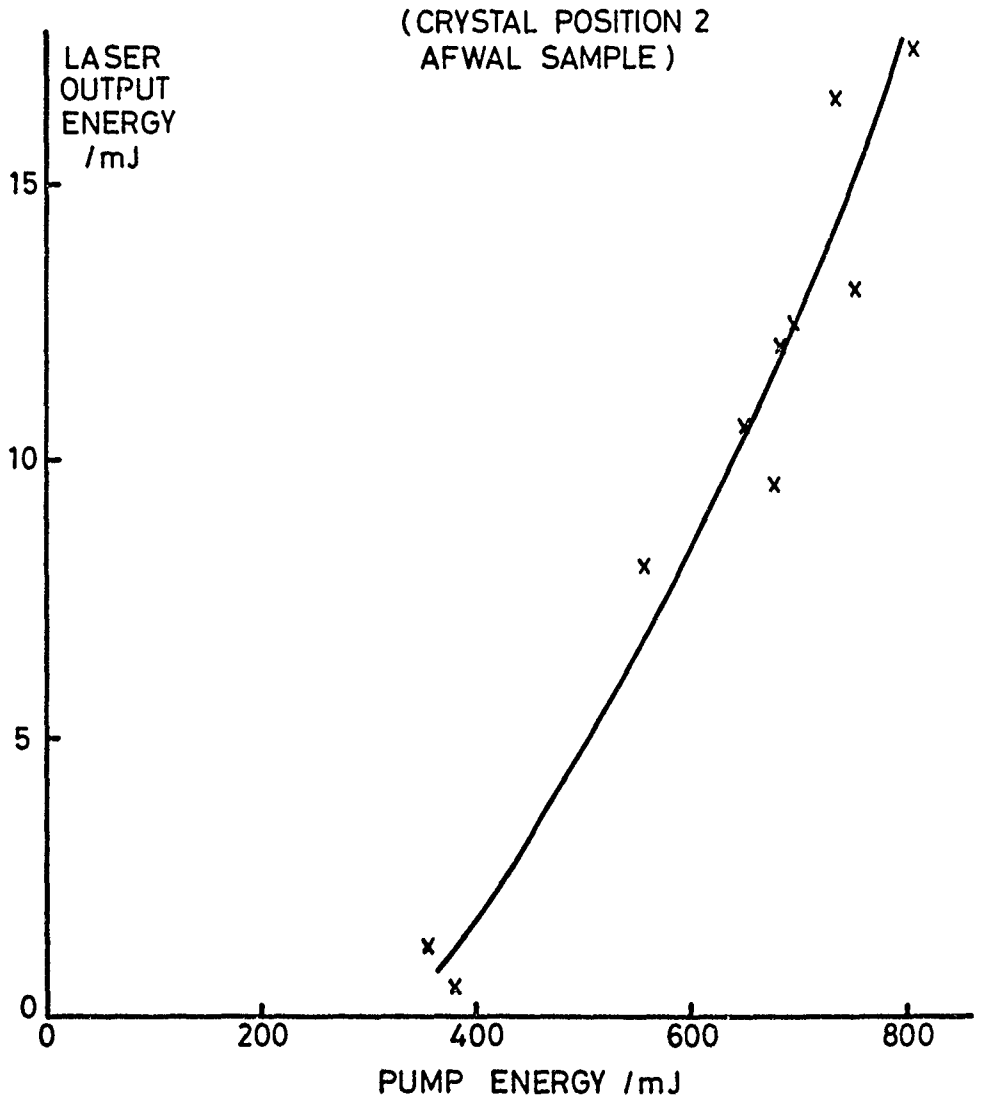

FIGURE. 4 Ti : SAPPHIRE LASING

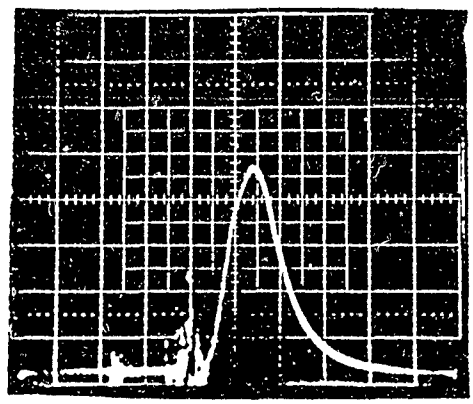

Figure.5 Pump Pulse
(2μs / div)

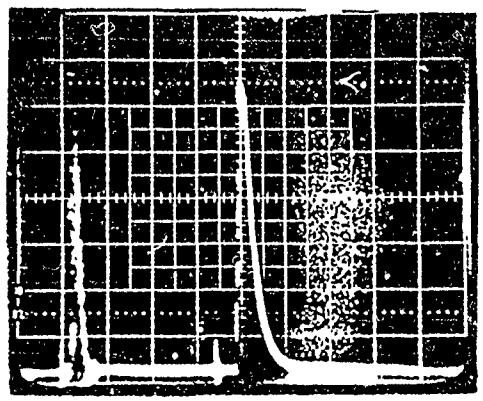

Figure.6 Sapphire laser output pulse (5μs / div)

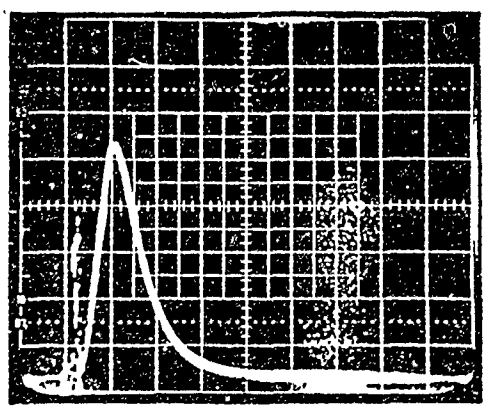

Figure.7 Titanium fluorescence during lasing (5μs / div)

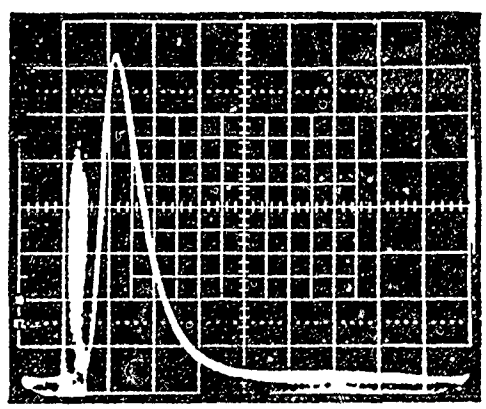

Figure.8 Titanium fluorescence with no lasing (5μs / div)

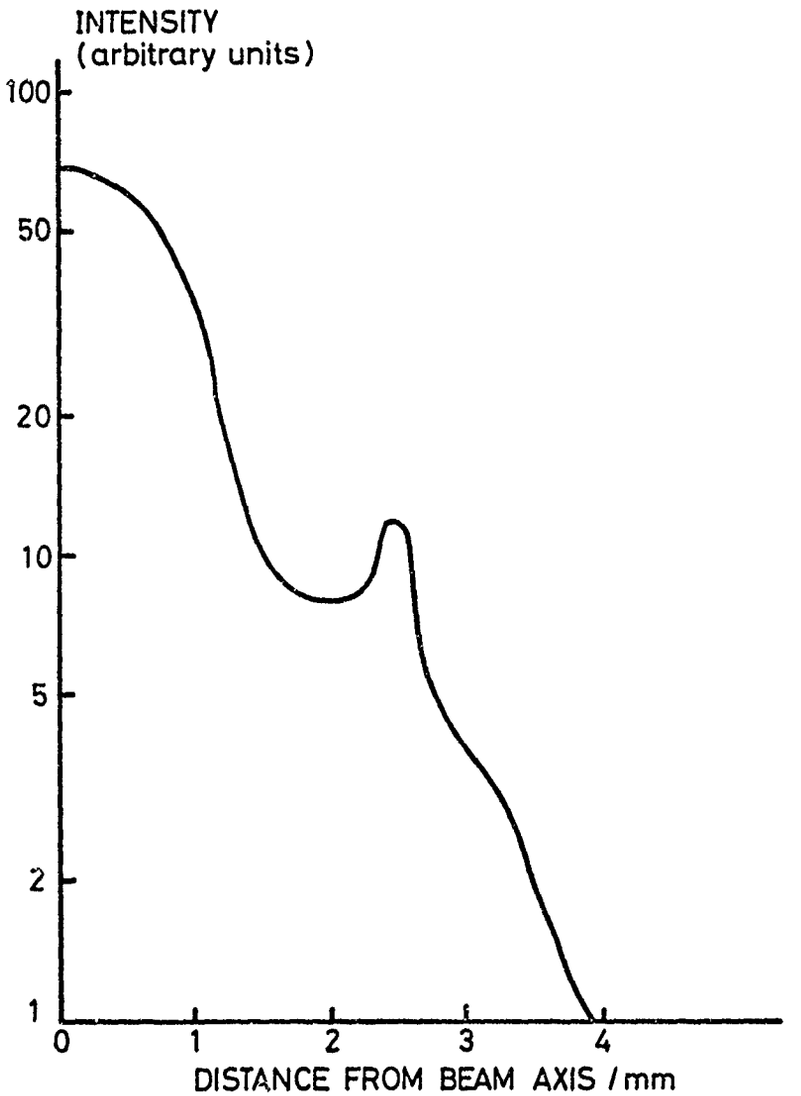

FIGURE.9 PUMP BEAM INTENSITY PROFILE
(In plane 55mm from focussed beam waist)

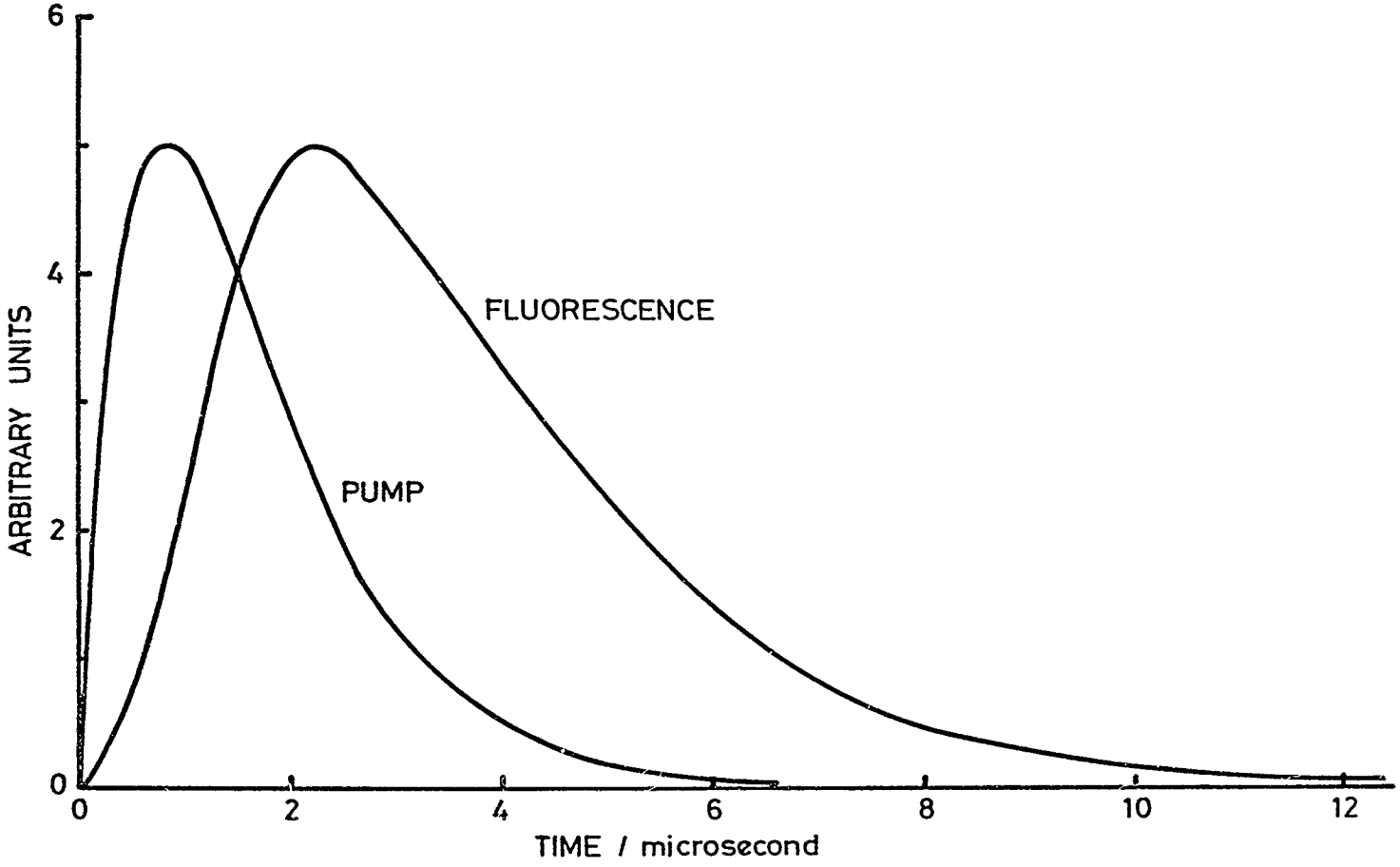

FIGURE. 10 PULSE SHAPES FOR Ti : SAPPHIRE PUMPING

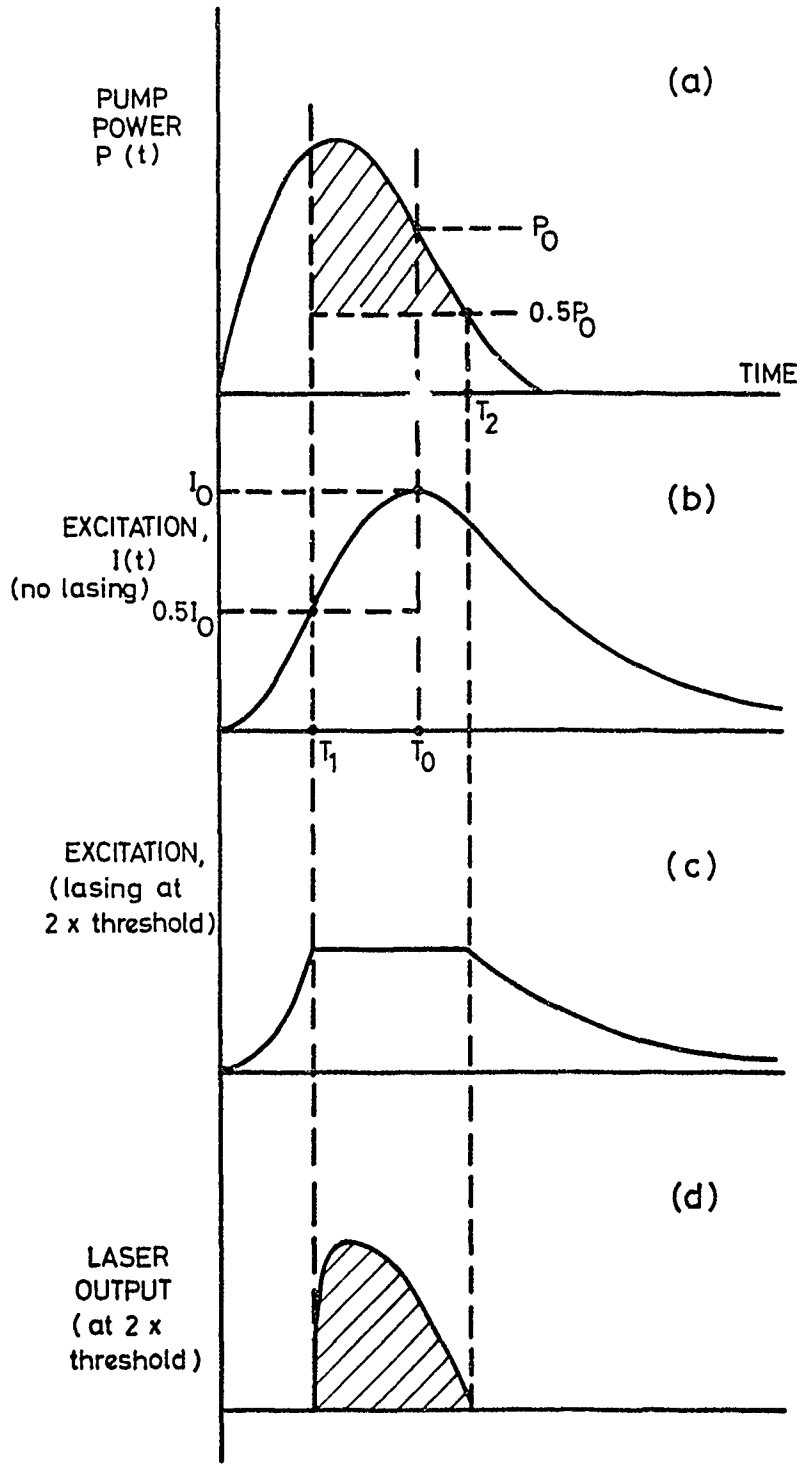

FIGURE.11 RELATION OF PUMP PULSE SHAPE TO LASER OUTPUT

DOCUMENT CONTROL SHEET

Overall security classification of sheet ..... UNCLASSIFIED .....

(As far as possible this sheet should contain only unclassified information. If it is necessary to enter classified information, the box concerned must be marked to indicate the classification eg (R) (C) or (S))

1. DRIC Reference (if known)	2. Originator's Reference	3. Agency Reference	4. Report Security Classification
	MEMO 4290		U/C

5. Originator's Code (if known)	6. Originator (Corporate Author) Name and Location
7784000	ROYAL SIGNALS AND RADAR ESTABLISHMENT ST ANDREWS ROAD, GREAT MALVERN WORCESTERSHIRE WR14 3PS
5a. Sponsoring Agency's Code (if known)	6a. Sponsoring Agency (Contract Authority) Name and Location

7. Title TITANIUM-DOPED SAPPHIRE LASERS WITH HIGH ENERGY PUMPING

7a. Title in Foreign Language (in the case of translations)

7b. Presented at (for conference papers) Title, place and date of conference

8. Author 1 Surname, initials	9(a) Author 2	9(b) Authors 3,4...	10. Date	pp. ref.
PAYNE M J P	LOWDE N A		1989.06	18

11. Contract Number	12. Period	13. Project	14. Other Reference

15. Distribution statement

UNLIMITED

Descriptors (or keywords)

continue on separate piece of paper

Abstract

A titanium-doped sapphire is pumped with up to 900 mJ of blue-green energy from a dye laser. 8% energy conversion to the near IR is demonstrated. The experimental input/output data agree well with calculations based on the measured characteristics of crystal and pump beam. Analysis of the conversion efficiency reveals the potential to achieve values of about 35% in optimised, but simple, devices. (AW)

380/48